ORIGINAL PAPER

R. González-Cruz · O. Solorza-Feria

Oxygen reduction in acid media by a $Ru_xFe_ySe_z(CO)_n$ cluster catalyst dispersed on a glassy carbon-supported Nafion film

Abstract Electrocatalytic oxygen reduction was studied on a $Ru_xFe_ySe_z(CO)_n$ cluster catalyst with Vulcan carbon powder dispersed into a Nafion film coated on a glassy carbon electrode. The synthesis of the electrocatalyst as a mixture of crystallites and amorphous nanoparticles was carried out by refluxing the transition metal carbonyl compounds in an organic solvent. Electrocatalysis by the cluster compound is discussed, based on the results of rotating disc electrode measurements in a 0.5 M H_2SO_4. A Tafel slope of -80.00 ± 4.72 mV dec^{-1} and an exchange current density of $1.1 \pm 0.17 \times 10^{-6}$ mA cm^{-2} was calculated from the mass transfer-corrected curve. It was found that the electrochemical reduction reaction follows the kinetics of a multielectronic ($n = 4e^-$) charge transfer process producing water, i.e. $O_2 + 4H^+ + 4e^- \rightarrow 2H_2O$.

Keywords Cathode · Electrocatalysis · Oxygen reduction

Introduction

Electrocatalysis of the molecular oxygen reduction reaction (ORR) continues to command a great deal of interest in modern electrochemistry owing to its technological importance in electrochemical devices such as cathode electrodes in fuel cells [1, 2], for which the four-electron oxygen reduction pathway is predominant in acid media [3, 4]. In the development of fuel cells operated at low temperature, small-size platinum and its alloys are used as electrodes. Therefore, there is an opportunity to develop novel active cathode catalysts in order to reduce the amount of precious metals used without losing performance from the present level. Clusters have different properties than the corresponding bulk solids. Interest in bimetallic cluster compounds as models for surface and catalytic reactions has lead to extensive research in this area [5, 6, 7]. Heteronuclear clusters are of particular interest since the differing reactivities of the metals may be explored in chemical transformations [8]. Ruthenium compounds synthesized at low temperature have been reported as good electrocatalysts which are able to transfer electrons via a ruthenium-centred mechanism for the ORR [9, 10, 11].

Our interest in the ORR at a ruthenium chalcogenide cluster electrode bearing iron atoms has lead us to investigate the feasibility of using this material as cathode electrodes in fuel cells [12]. The main reasons for incorporating selenium into ruthenium and other transition metal cluster compounds is to improve the stability of the new compound as well as to obtain an enhancement of the electrocatalytic activity due to synergistic effects.

The aim of this work is to present the synthesis and characterization of a bimetallic chalcogenide cluster catalyst prepared by reacting the transition metal carbonyl compounds with elemental selenium in 1,2-dichlorobenzene for 20 h. The study of the electrocatalytic activity of the cluster compound supported on Vulcan carbon and dispersed into a Nafion film also constitutes part of this work.

R. González-Cruz · O. Solorza-Feria (✉)
Departamento de Química,
Centro de Investigación y de Estudios Avanzados del IPN,
A. Postal 14-740, 07360, DF, Mexico
E-mail: osolorza@mail.cinvestav.mx

Experimental

Catalyst preparation

The cluster catalyst was synthesized by reacting $Ru_3(CO)_{12}$ (88.33 mg, 0.139 mmol) with $Fe_3(CO)_{12}$ (70 mg, 0.139 mmol) and elemental selenium (32.9 mg, 0.417 mmol) in 1,2-dichlorobenzene (bp≈180 °C). The preparation was performed under refluxing conditions with continuous stirring in an inert atmosphere for 20 h. After cooling to room temperature, the reaction mixture

was filtered and the resulting powder was washed with acetone and methanol. Afterwards the powder was placed in a furnace at 120 °C for 1.5 h in order to dry it completely. The resulting dark and fine powder was used for optical characterization and electrochemical measurements.

Chemical and physical characterization

IR spectra were measured on a FTIR Perkin-Elmer 16F spectrometer. Samples for this technique were prepared by thoroughly mixing the catalyst powder with dry KBr (Aldrich).

The surface morphology of the cluster catalyst was examined using a scanning electron microscope (SEM, Jeol 3600), equipped with an energy dispersive X-ray microanalysis unit (EDAX), to determine the chemical composition at different points of the sample. Catalyst particle size distribution was determined with a transmission electron microscope (TEM, Jeol 2010), at 200 kV accelerating voltage. The XRD technique was used for the determination of the average particle size. X-ray diffractions were recorded by a Siemens D5000 diffractometer for powders, equipped with a Cu K_α radiation source.

Electrochemical characterization

An alcoholic solution with 5 wt% Nafion was purchased from Aldrich and the glassy carbon (GC) rod was purchased from Sygradur. Discs with a cross-sectional area of 0.196 cm^2 and thickness of 5 mm were used as a support for the thin films and used as working electrodes. Each disc was placed in a cup of an electrode holder made of Nylamid with a stainless-steel bottom. The GC electrode surface was modified as follows: to an alcoholic solution (0.22 mL) containing 8 μL of 5 wt% Nafion (Du Pont, 1100 EW), 1 mg of the catalyst and 0.2 mg of Vulcan carbon XC-72R (Cabot) were added. The resulting mixture was sonicated for 2 min and deposited onto the GC surface. A thin film of 0.4 μm thickness was estimated, taking into account the amount of electrocatalyst and the density of the Nafion [13].

The electrochemical measurements were performed by using the conventional single compartment of a three-electrode array. The cyclic voltammetry and the rotating disc electrode (RDE) studies were carried out at 25 °C. A platinum mesh was used as the counter electrode and Hg/Hg$_2$SO$_4$/0.5 M H$_2$SO$_4$ (MSE = 0.68 V/NHE) as the reference electrode. All the potentials are referred to NHE. A potentiostat (EG&G, model 273A) was used for the steady-state experiments. Hydrodynamics experiments were recorded in the rotation rate range 100–1600 rpm at 5 mV/s. At least three electrodes were prepared from different syntheses. A 0.5 M H$_2$SO$_4$ (pH 0.3) aqueous solution was used as the electrolyte, prepared from doubly distilled water. Prior to the electrochemical measurements, the solution was degassed with nitrogen for the working electrode activation. The electrode activation was carried out by scanning the potential between 0.83 V and −0.03 V/NHE for 20 min. Afterwards, the electrolyte was saturated with oxygen whose flux was maintained above the electrolyte during the measurements.

Results and discussion

Catalyst characterization

The preparation of the $Ru_xFe_ySe_z(CO)_n$ cluster catalyst by thermal condensation is not a selective synthesis, and a mixture of lower- and higher-nuclearity clusters by following this technique is formed [14]. The real composition of the synthesized powder has not yet been determined. Figure 1 shows the FTIR spectrum of a KBr pellet of the synthesized $Ru_xSe_z(CO)_n$, $Ru_xFe_y(CO)_n$ and $Ru_xFe_ySe_z(CO)_n$ cluster catalysts. Bands observed at 2000 cm^{-1} and 2070 cm^{-1} in $Ru_xSe_z(CO)_n$ and $Ru_xFe_y(CO)_n$ correspond to terminal carbonyls and a broad band in the range 1550–1650 cm^{-1} was assigned to the face-bridging carbonyls $[\mu_3\text{-}(CO)]$, as reported for similar clusters [14]. A band in the same range of 1550–1650 cm^{-1} was also observed in the $Ru_xFe_ySe_z(CO)_n$ cluster, while this cluster also showed a band at 1780 cm^{-1} which can be assigned to the edge-bridging carbonyl $[\mu_2\text{-}(CO)]$; a band at 1555 cm^{-1} is probably due to σ/π-bridge carbonyls, and prominent

Fig. 1 FTIR spectra of the synthesized powder after 20 h of cluster catalyst preparation
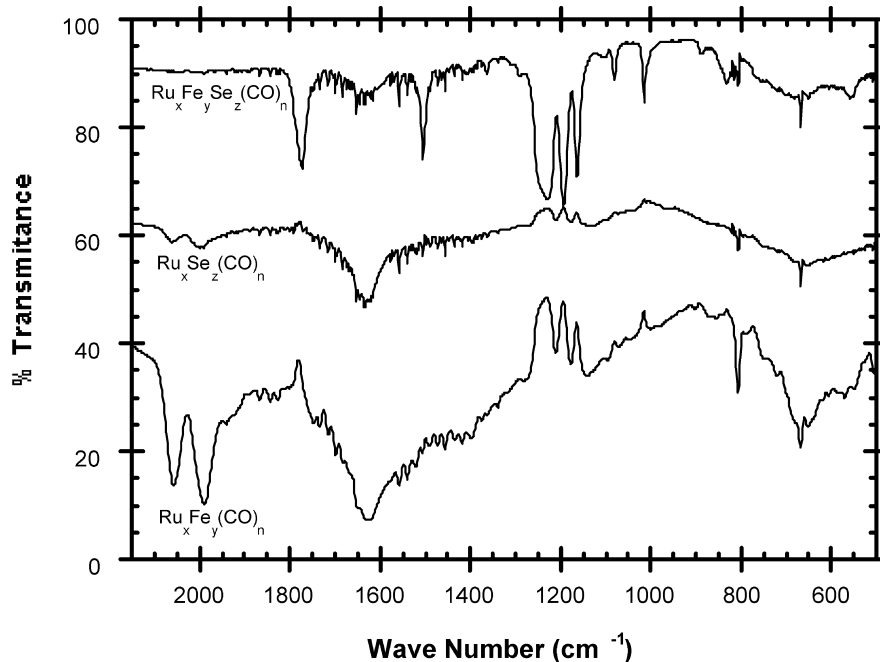
bands observed in the region 1150–1250 cm^{-1} were assigned to hydride bridges of the type M-H-M, as has been reported [15, 16].

TEM of the synthesized $Ru_xFe_ySe_z(CO)_n$ cluster catalyst (Fig. 2) shows metallic nanoparticles of diameter under 5 nm, incorporated into an amorphous layer of the particle surface. Similar images were obtained with the products from the thermal condensation reaction between the Ru and Fe transition carbonyl compounds in 1,6-hexanediol [17]. The particle sizes suggest that the synthesized cluster compound could be a suitable material for use in electrocatalysis. The average EDAX microanalysis gave a ca. 1.4:1 Ru:Fe atomic ratio and a 1.9:1 Ru:Se atomic ratio. The X-ray diffraction pattern of the $Ru_xFe_ySe_z(CO)_n$ cluster catalyst is shown in Fig. 3. The lack of sharp peaks rules out the presence of crystallites. From the extent of the line broadening at $2\theta \approx 43°$, the average crystallite size of metallic ruthenium is estimated to be 3.5 nm with the use of the Scherrer equation after background subtraction. The broad signal observed at about 10–20° is probably due to amorphous states of compounds produced during the chemical condensation reaction. The analytical results confirm that the chemical preparation procedure is not a selective technique for the preparation of only a nanocrystalline electrocatalyst, because a nanocrystalline-amorphous compound is produced. The precise structure and the real composition have not yet been determined owing to the polynuclearity and to the amorphous portion of the synthesized compound, which made separation by the traditional technique of chemical quantification difficult. However, since carbonyls are contained in the synthesized electrocatalyst, their estimated composition should be $Ru_xFe_ySe_z(CO)_n$.

Fig. 2 TEM picture of the as-synthesized $Ru_xFe_ySe_z(CO)_n$ cluster catalyst

Cyclic voltammetry and RDE study of the oxygen

Cyclic voltammograms of the $Ru_xFe_ySe_z(CO)_n$ cluster catalyst incorporated into a Nafion film were recorded in a small potential region, 0.86–0.75 V vs. NHE (Fig. 4), where a dependence of non-faradaic currents on the sweep rate was obtained. These voltammograms were

Fig. 3 Powder XRD pattern of the $Ru_xFe_ySe_z(CO)_n$ cluster catalyst as synthesized in 1,2-dichlorobenzene for 20 h
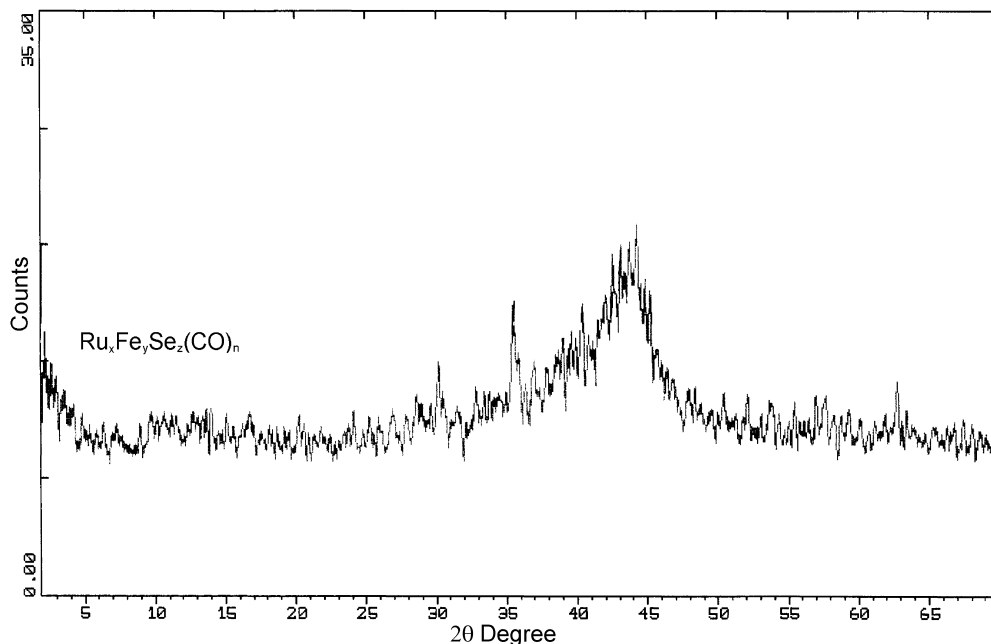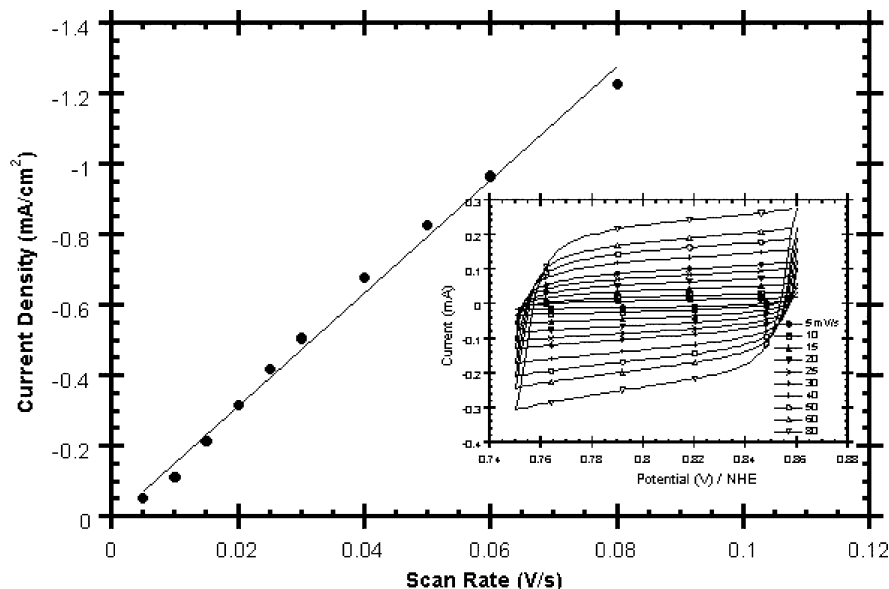
recorded after scanning the electrode potential between
0.8 V and 0.0 V vs. NHE at 50 mV/s for 10 min, in
order to eliminate impurities and oxides, until a defined
capacitive current was reached. A good linear relation-
ship was observed in the range 5–80 mV s^{-1}. From the
slope of the linear region of the double layer charging
current versus sweep rate measured at 0.80 V, the
capacitance of the electrode/solution interface ($C = dq/
dE = di/dv$) was calculated, normalizing the capacitance
to the geometrical surface area. An average value of
14.92 ± 0.53 μF cm^{-2} was obtained.

Steady-state current-potential curves at six different
rotation rates produced by the molecular oxygen reduc-
tion at the $Ru_xFe_ySe_z(CO)_n$ cluster catalyst incorporated

into a Nafion film, corrected from the non-faradaic
current, are shown in Fig. 5. Oxygen diffuses into the
Nafion phase and reacts simultaneously at the catalyst
interfaces. As shown in this figure, in the region between
0.85 V and 0.73 V vs. NHE, no significant variation of
the currents with the rotation rates was observed, char-
acteristic of charge-transfer kinetics control. Mixed
control in the range 0.75–0.60 V vs. NHE and, at higher
cathodic potentials, a dependence of a well-defined lim-
iting current on rotation rate is observed. With increasing
rotation speed, limiting currents were increased due to
the increase of oxygen diffusion through the electrode
surface. The Koutecky-Levich plots corresponding to the
experimental values of Fig. 5 are shown in Fig. 6, using
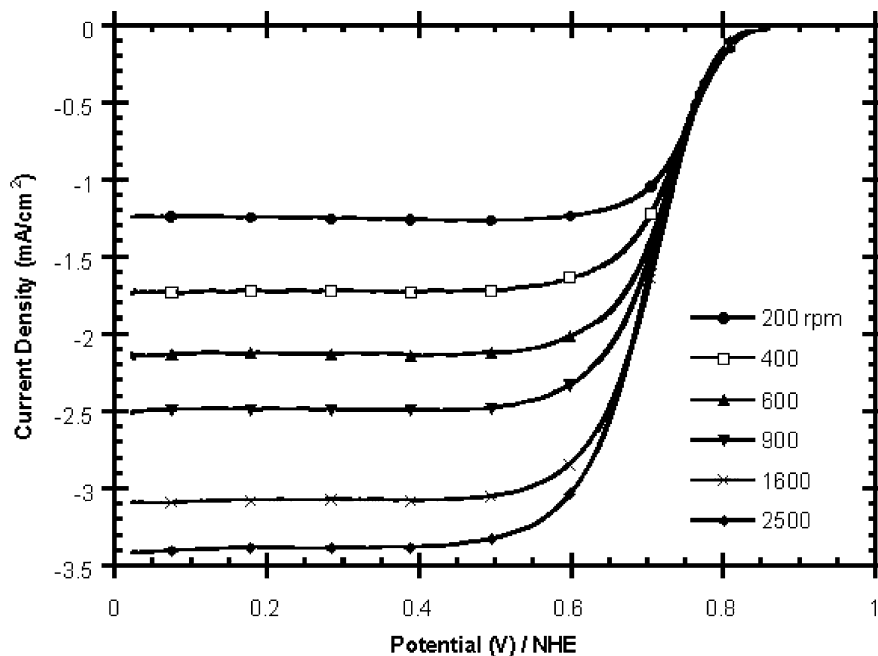
the following first-order reaction kinetics and taking into account the Nafion thin film [13, 18]:

$$\frac{1}{i} = \frac{1}{i_k} + \frac{1}{B\omega^{1/2}} \qquad (1)$$

where i is the measured current, i_k the kinetic contribution to the current and ω is the electrode rotation rate. The theoretical value of the Levich slope, B, is evaluated from Eq. 2:

$$B = 0.2nFC_oD_o^{2/3}v^{-1/6} \qquad (2)$$

where 0.2 is a constant used when ω is expressed in revolutions per minute, n is the number of electrons related to the oxygen reduction reaction, F the Faraday constant (96,500 C mol^{-1}), C_o is the concentration of oxygen in 0.5 M H_2SO_4 (1.1×10^{-6} mol cm^{-3}), D_o is the diffusion coefficient of oxygen in the solution (1.4×10^{-5} cm^2 s^{-1}) and v is the kinematic viscosity of the sulfuric acid (1.7×10^{-2} cm^{-2} s^{-1}) [19]. The theoretical value of B was found to be 0.106 mA s$^{1/2}$ with $n=4$. From the slope of Fig. 6 the experimental value of B was found to be 0.101 mA s$^{1/2}$ and is close to the theoretical value. The satisfactory agreement between these two values suggests that the kinetics is favorable toward a multielectron charge transfer process ($n=4e^-$) leading to water formation, i.e. $O_2+4H^++4e^- \rightarrow 2H_2O$. Studies in progress by the rotating ring-disk electrode technique will give us more information about the kinetics. Figure 7 shows the potential dependence of the kinetic density currents corrected for diffusion effects (given as Tafel plots) of the $Ru_xFe_ySe_z(CO)_n$ cluster catalyst incorporated into a Nafion film and that of the $Ru_xSe_y(CO)_n$ and $Ru_xFe_y(CO)_n$ electrocacalysts analyzed under the same experimental conditions. It is clear that the electrocatalytic activity for oxygen reduction of the

bimetallic combination improves with the addition of selenium. The success of the enhanced electrocatalytic activity could be associated with the synergistic effect of the dispersed mixed amorphous phases of lower and higher cluster materials whose electronic interactions improve the electrode kinetic surface. The favorable influence of selenium on the Ru-based catalysts for oxygen reduction in acid electrolytes could also be attributed to the modification of the catalytic active centre by selenium taking the position of a CO group, altering the electronic properties of the active centre and facilitating the electron transfer [20]. It is clear that the electrochemical ORR must depend on the coordinating ability of the reactive centres of both the Ru and Fe electrocatalysts which react interfacially with the adsorbed oxygen via the transition metal d-states. This statement and possible implications in the subsequent electron transfer process have been discussed by Tributsch and co-workers [20, 21]. The kinetic results obtained from the Tafel slope deduced in the range 0.70–0.82 V/NHE of Fig. 7 are collected in Table 1. The Tafel slope of −0.117 V with the $Ru_xFe_y(CO)_n$ electrocacalyst corresponds to the transfer of the first electron to the adsorbed oxygen as the rate-determining step:

$$(O_2)_{ads} + H^+ + e^- \rightarrow (HO_2)_{ads} \qquad (3)$$
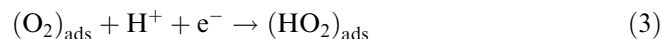
The Tafel slope is used as one of the most frequently diagnostic criteria in the elucidation of the reaction mechanism. In most cases, slope values such as −0.060 and −0.120 V can be easily explained. The existence of these two slopes is explained in terms of the coverage of the electrode surface by adsorbed oxygen, which follows a Temkin isotherm (high coverage) at low overpotentials and a Langmuir isotherm (low coverage) at higher overpotentials [22, 23]. However, a Tafel slope value of

Fig. 6 i^{-1} vs. $\omega^{-1/2}$ plots at various electrode potentials for oxygen reduction obtained from Fig. 5
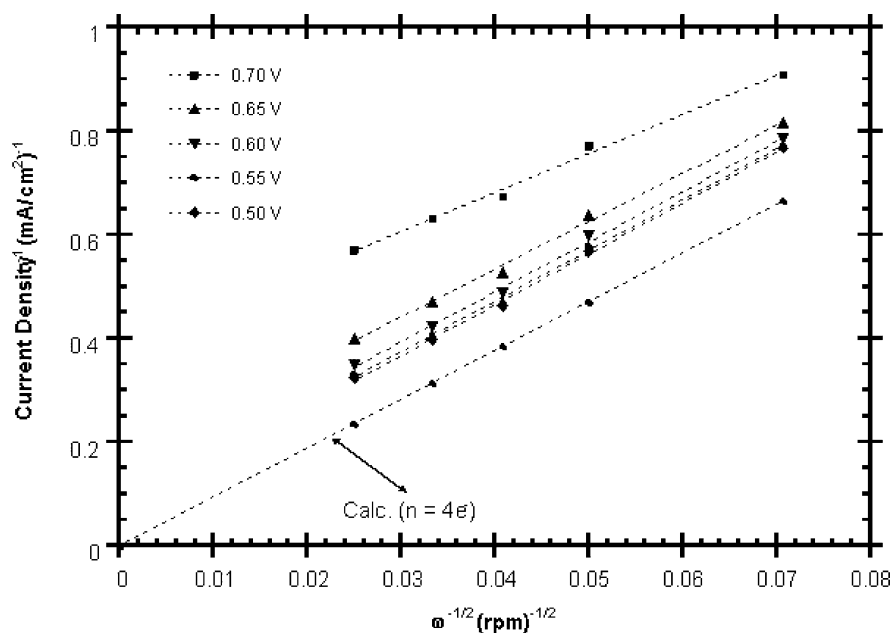
Fig. 7 Mass-transfer-corrected Tafel plots for oxygen reduction on various Ru-based cluster catalysts in 0.5 M H_2SO_4
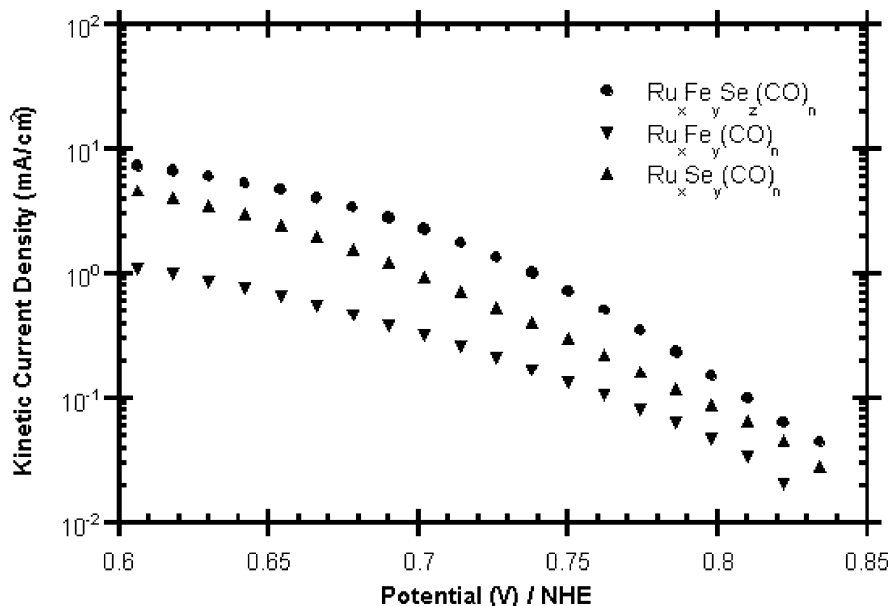

Table 1 Kinetic parameters deduced from the mass-transfer-corrected Tafel plots of the ORR in 0.5 M H_2SO_4

Sample	Tafel slope, $-b$ (mV/dec)	Transfer coefficient, α	i_o (mA/cm^2) $\times 10^{-6}$	i (mA/cm^2) at $E = 0.7$ V vs. NHE
$Ru_xSe_z(CO)_n$	87.73 (90.00)[a]	0.67	1.65	1.05
$Ru_xFe_y(CO)_n$	117.02 ± 2.62	0.51 ± 0.01	13.54 ± 3.98	0.32
$Ru_xFe_ySe_z(CO)_n$	80.00 ± 4.72	0.74 ± 0.01	1.1 ± 0.17	2.28

[a]From [26]

−0.080 V, determined for the oxygen reduction on the $Ru_xFe_ySe_z(CO)_n$ cluster catalyst, suggests a rather complex reaction mechanism which is very difficult to explain.

The values of the exchange current density presented in Table 1 are similar for the Ru-based catalysts supported on Nafion-modified electrodes, and also are similar to highly dispersed Pt on high-surface-area carbon used in fuel cells [24, 25]. In Table 1 is also seen the influence of iron in the current density at 0.7 V vs. NHE, when it is incorporated in the ruthenium-selenium catalyst compound. From the deduced electrochemical results, we suggest that the $Ru_xFe_ySe_z(CO)_n$ cluster catalyst could be considered in the fabrication of membrane electrode assemblies and for testing as a cathode for the ORR in a polymer electrolyte fuel cell.

Conclusions

The present study has shown that the incorporation of Fe into the $Ru_xSe_y(CO)_n$ cluster catalyst produces a synergistic interaction enhancing the electron transfer rate for the ORR. The performance of the Ru_xFe_y-$Se_z(CO)_n$ cluster electrocatalyst dispersed into a Nafion film, and coated on a GC electrode, shows considerable stability in sulfuric acid media and could be considered as a cathode in a proton exchange membrane fuel cell.

References

1. Kordesh K, Simader G (1996) Fuel cells and their applications. VCH, New York, pp 1–7
2. Williams MC (ed) (2000) Fuel cell handbook, 5th edn. US Department of Energy, Washington, pp 1–37
3. Adzic R (1998) In: Lipkowski J, Ross P.N (eds) Electrocatalysis. Wiley-VCH, New York, pp 197–242
4. Kinoshita K (1992) Electrochemical oxygen technology. Wiley, New York, p 19
5. Muetterties EL, Rhodin TN, Band E, Brucker CF, Pretzer WR (1979) Chem Rev 79:91
6. Ross PN (1998) In: Lipkowski J, Ross PJ (eds) Electrocatalysis. Wiley-VCH, pp 43–74
7. Soriaga MP (1990) Chem Rev 90:771
8. Braunstein P, Rosé J (1999) In: Braunstein P, Oro LA, Raithby PR (eds) Metal clusters in chemistry, vol 2. Wiley-VCH, New York, pp 616–677
9. Alonso-Vante N, Bogdanoff P, Tributsch H (2000) J Catal 190:240
10. Le Run V, Garnier E, Pronier S, Alonso-Vante N (2000) Electrochem Commun 2:475
11. Duron S, Rivera-Noriega R, Poillerat G, Solorza-Feria O (2001) J New Mater Electrochem Syst 4:17
12. González-Cruz R, Solorza-Feria O, Rivera-Noriega R (2000) Proc SIBAE, Oaxaca, Mexico, ENE015:1
13. Watanabe M, Igarashi H, Yoshioka K (1995) Electrochim Acta 40:329
14. Mingos DMP, Wales DJ (1990) Introduction to cluster chemistry. Prentice Hall, Englewood Cliffs, NJ, p 205
15. Howard MW, Skinner P, Bhardwa RK, Jayasooriya UA, Powel DB, Sheppard N (1986) Inorg Chem 25:2846

16. Jayasooriya UA, Stotesbury SJ, Grinter R, Powell DB, Sheppard N (1986) Inorg Chem 25:2853
17. Rivera-Noriega R, Castillo-Hernández N, Soto-Guzmán AB, Solorza-Feria O (2002) Int J Hydrogen Energy 27:457
18. Schmidt TJ, Gasteiger HA, Stab GD, Urban PM, Kolb DM, Behm RJ (1998) J Electrochem Soc 145:2354
19. Hsueh K, Gonzalez ER, Srinivasan S (1983) Electrochim Acta 28:691
20. Bron M, Bogdanoff P, Fiechter S, Dorbandt I, Hilgendorff M, Schulenburg H, Tributsch H (2001) J Electroanal Chem 500:510
21. Tributsch H, Bron M, Hilgendorff M, Schulenburg H, Dorbandt I, Eyert V, Bogdanoff P, Fichter S (2001) J Appl Electrochem 31:739
22. Sepa DB, Vojnovic MV, Damjanovic A (1981) Electrochim Acta 26:781
23. Damjanovich A, Brusic V (1967) Electrochim Acta 12:615
24. Perez J, Gonzalez ER, Ticianelli EA (1998) J Electrochem Soc 145:2307
25. Perez J, Gonzalez ER, Ticianelli EA (1998) Electrochim Acta 44:1329
26. Bron M, Bogdanoff P, Fiechter S, Hilgendorff M, Radnik J, Dorbandt I, Schulenburg H, Tributsch H (2001) J Electroanal Chem 517:85